



HAL
open science

On the fatigue life prediction of CFRP laminates using the Electrical Resistance Change method

A. Vavouliotis, A. Paipetis, V. Kostopoulos

► **To cite this version:**

A. Vavouliotis, A. Paipetis, V. Kostopoulos. On the fatigue life prediction of CFRP laminates using the Electrical Resistance Change method. *Composites Science and Technology*, 2011, 71 (5), pp.630. 10.1016/j.compscitech.2011.01.003 . hal-00730307

HAL Id: hal-00730307

<https://hal.science/hal-00730307>

Submitted on 9 Sep 2012

HAL is a multi-disciplinary open access archive for the deposit and dissemination of scientific research documents, whether they are published or not. The documents may come from teaching and research institutions in France or abroad, or from public or private research centers.

L'archive ouverte pluridisciplinaire **HAL**, est destinée au dépôt et à la diffusion de documents scientifiques de niveau recherche, publiés ou non, émanant des établissements d'enseignement et de recherche français ou étrangers, des laboratoires publics ou privés.

Accepted Manuscript

On the fatigue life prediction of CFRP laminates using the Electrical Resistance Change method

A. Vavouliotis, A. Paipetis, V. Kostopoulos

PII: S0266-3538(11)00031-5
DOI: [10.1016/j.compscitech.2011.01.003](https://doi.org/10.1016/j.compscitech.2011.01.003)
Reference: CSTE 4898

To appear in: *Composites Science and Technology*

Received Date: 18 August 2010
Revised Date: 30 December 2010
Accepted Date: 6 January 2011

Please cite this article as: Vavouliotis, A., Paipetis, A., Kostopoulos, V., On the fatigue life prediction of CFRP laminates using the Electrical Resistance Change method, *Composites Science and Technology* (2011), doi: [10.1016/j.compscitech.2011.01.003](https://doi.org/10.1016/j.compscitech.2011.01.003)

This is a PDF file of an unedited manuscript that has been accepted for publication. As a service to our customers we are providing this early version of the manuscript. The manuscript will undergo copyediting, typesetting, and review of the resulting proof before it is published in its final form. Please note that during the production process errors may be discovered which could affect the content, and all legal disclaimers that apply to the journal pertain.



On the fatigue life prediction of CFRP laminates using the Electrical Resistance Change method

A. Vavouliotis¹, A. Paipetis² and V. Kostopoulos^{*1}

¹ Applied Mechanics Laboratory,

Department of Mechanical Engineering and Aeronautics, University of Patras, Patras University

Campus, GR-26500, Patras, Greece

² Department of Materials Science & Engineering, University of Ioannina, GR-45110, Ioannina,
Greece

*Corresponding author:

e-mail: kostopoulos@mech.upatras.gr, tel: +30 2610 969443

Submitted for publication in Composite Science and Technology

DECEMBER 2010

Abstract

The electromechanical response (Electrical Resistance Change method) as a damage index of quasi-isotropic Carbon Fiber Reinforced (CFRPs) laminates under fatigue loading was investigated. The effect of dispersed Multi-Wall Carbon Nanotubes (MWCNT) into the epoxy matrix was additionally evaluated and compared with neat epoxy CFRPs. The longitudinal resistance change of the specimens was monitored throughout the fatigue experiment. Three different stress levels were tested. The frequency and the ratio (R) of the minimum applied load (stress) to the maximum applied load (stress) were kept constant for the different stress levels. The temperature of the specimen was also monitored throughout the process in order to deduce its effect on the electrical resistance of the specimen. The electrical behavior of the quasi-isotropic CFRP deviated from the commonly observed electrical response of unidirectional or cross-ply CFRPs due to the presence of the 45° layers. During initial stages of loading the resistance drops and afterwards it follows a positive slope up to final fracture. This repeatable pattern was observed for both the neat and the CNT-doped specimens, with the latter having smoother electrical recordings. The effect of temperature was calculated to be limited for the specific material and test/measurement configuration. The electromechanical response was correlated to stiffness degradation and acoustic emission findings enabling the identification of the specific regions during the fatigue life referring to specific mechanisms of damage accumulation. More specifically the experimental results revealed that the occurrence of the initial drop of the electrical resistance is linked with the occurrence of the Characteristic Damage State (CDS), associated with a specific percentage of stiffness reduction. This finding was used in order to predict the remaining life independently from the applied stress level with a high degree of confidence, assuming a constant stress level throughout the whole lifetime. The remaining life prediction for the CNT-doped specimens had higher coefficient of confidence (R^2).

Keywords: **D.** Fatigue Damage Monitoring, **B.** Critical Damage State, **D.** Electrical Resistance Change, **A.** Carbon nanotubes, **A.** CFRP.

1. Introduction

Continuous health monitoring of composite structures can contribute towards the enhancement of safety and operational cost minimization by optimizing maintenance protocols of aerospace structures. Non-destructive monitoring of the damage developed in continuous carbon fiber reinforced composites during mechanical/operational loading is a key issue in many applications, especially in the field of aerospace structures. The optimal way to proceed for structural health monitoring is to use the material itself as sensor of its own damage. To this end, the electrical resistance change (ERC) method is appropriate since it employs the electrical conductivity, an inherent material property, to identify internal damage. Electrical conduction in CFRPs is realized directly through the conductive carbon fibers but also indirectly through the electrical contacts between the neighboring fibers. The ERC method does not require expensive equipment for instrumentation and does not cause any deterioration of the structure under monitoring. Furthermore the structural weight is not changed.

The ERC method was initially proposed by Baron and Schulte in 1988 and has been studied for the last twenty years by various researchers worldwide [1-4]. In the case of CFRPs, it has been proven that the electrical resistance, the mechanical deformation and damage are interconnected. This conclusion has been verified for various types of mechanical loadings (quasi-static, fatigue, impact etc) but mainly for unidirectional or orthotropic CFRP materials. However, there exist limited studies that employ the ERC method under dynamic mechanical loading and especially fatigue with a view to life prediction. For this reason, the principal aim of this study was to investigate the electromechanical response (ERC method) in order to extract appropriate damage indices for quasi-isotropic CFRP laminates under fatigue loading. This was performed with a view to use them to predict the remaining fatigue life of the CFRP.

In parallel, the effect of the dispersion of Multi-Wall Carbon Nanotubes (MWCNT) in the CFRP epoxy matrix was evaluated and compared with neat epoxy CFRPs. The incorporation of the nanotechnology in structural composites is very promising as it may offer increased damage tolerance and additional functionalities, Nano-scale fillers such as carbon nanotubes (CNTs) have

been placed recently in the epicenter of composite research as modifiers of the polymer matrices of the CFRPs [5-7]. Taking into consideration their high aspect ratio, large surface area and excellent electrical properties, they may offer the benefits of an additional reinforcing phase acting at the nano-scale. Recent studies on unidirectional CFRP composites [8-10] reported that the CNT inclusion improved the transverse conductivity rendering the UD composite more electrically isotropic. Moreover the resistance change due to monotonic and cyclic tensile loading using was more pronounced for the laminates with the modified matrices. Using a 2 surface probe/4 wires electrode configuration the presence of the electrically conductive CNT network acted as a direct sensor of matrix related damage phenomena, which was complementary to changes related to failure of the reinforcing phase. A good correlation between fatigue damage and environmental degradation with electrical resistance has been also been reported [11-12].

2. Experimental

2.1 Manufacturing

Quasi-isotropic CFRP composites were manufactured by wet lamination and cured in an autoclave. The quasi-isotropic lamination sequence was $[0, +45, 90, -45]_{2s}$. A unidirectional carbon fibre layer produced by Wela, Germany, was utilized, (weight 160 g/m^2). The epoxy matrix was the aerospace approved system Araldite LY564/Aradur HY2954 by Huntsman Advanced Materials, Switzerland. The curing profile included one hour at 80°C and eight hours at 140°C . Two types of CFRP laminates were manufactured. A conventional (reference) composite that employed plain epoxy as a matrix and a nano-modified composite where a small weight percentage of MWCNTs (0.5%) was employed to modify the same epoxy system.

The MWCNTs were supplied by ARKEMA, France and were produced by catalyzed CVD (98% purity). Their diameter ranged from 10–15 nm and they were more than 500 nm long i.e. their aspect ratio was approximately 30-50. The dispersion of the MWCNTs in the epoxy was performed using a Torus Mill device (VMA Getzmann GmbH). The Torus Mill reduced the nano-particle agglomerates as it introduced high shear forces by a high speed rotating disc and in conjunction with a milling effect generated by zirconium dioxide beads of 1.2-1.7 mm in diameter. The

compound was stirred under vacuum to avoid air inclusion. The mixing was performed at 2000 rpm for 3 h. The CNT content was 0.5 % wt.

The neat and the nano-doped resin were used for the manufacturing of the respective CFRP composite panels as described earlier. The final thickness of the CFRPs was 2.4 ± 0.1 mm. The volume fraction of both panels was measured using a light microscope at approximately 58%. The void content was negligible using the same method. Tensile specimens were cut from the composite panels using a water-jet. The specimens were subsequently placed in an oven at 50°C for 20 hours in order to eliminate any humidity. The specimens were 250 ± 0.5 mm long by 20 ± 0.2 mm wide, according the ASTM-D3039 and ASTM-D3479 standards.

2.2 Testing Procedure

Prior to fatigue, quasi static tensile tests (ASTM D-3039) were performed in order to define the ultimate strength (σ_{uts}) values that were employed for the definition of the fatigue stress levels. The results showed that the ultimate strength was 530 ± 15 MPa for the conventional CFRPs and 495 ± 22 MPa for the nanomodified CFRPs. All chosen stress levels (80%, 70% and 60% of σ_{uts}) were higher than the endurance fatigue limit so as to ensure the fracture of the specimen. The chosen fatigue parameters were; cyclic frequency $f = 5$ Hz, stress ratio $R = 0.1$. All tests were performed using an INSTRON universal testing machine equipped with 100 kN load cell. The measurement of electrical resistance was performed using a digital multimeter (KEITHLEY-DMM-2002). As depicted in Figure 1, this study used a four (4) wire electrical resistance measuring method with a two (2) probe/electrodes topology. The 4 wire method, was selected to eliminate the parasitic resistance of the cables. The topology of the measurement covered the complete volume of the specimen at the longitudinal axis of the specimen. Therefore, the electrodes placed covered almost all the gripping area of the specimens together with the free cross sections. For optimum electrical contact, the top and bottom cross-section of the specimen were coated with electrically conductive paint (silver loaded paint). The electrodes were formed using straps of electrically conductive adhesive tape (silver loaded adhesive tape), which were wrapped around the gripping area and the free cross sections so as to achieve good electrical contact with the conductive paint. The emery

cloth, which was proposed as tab material by the fatigue standard, served also as electrical insulation of the specimen from the grips. Additionally, two thermocouples (type K) for recording the temperature of the specimen during fatigue were placed on the surface of each specimen at an 80 mm distance apart (Figure 1). A thermo-conductive paste was used for optimum thermal contact. All parameters (electrical resistance, temperature, load, displacement, time, etc) were recorded simultaneously using a central logging system (Figure 2). The sampling frequency of the system was 25 Hz, so as to allow for 5 readings of electrical resistance per fatigue cycle for the selected frequency of 5 Hz.

3. Results

As has been confirmed in previous studies [10-11], the electrical resistance monitoring system was able to follow directly the applied strain cycle during the complete duration of tension-tension fatigue tests. As can be seen in Figure 3, a fivefold sampling rate compared to the fatigue frequency enabled real time strain monitoring. Additionally (Figure 4) the mean –stress/cycle free- electrical resistance change (or the relative resistance change at zero load for each fatigue cycle) is plotted against the number of fatigue cycles. This relative resistance change was recorded until fracture for all tested specimens and revealed a repeated pattern of electro-mechanical behavior during fatigue loading: during initial stages of loading the resistance drops and afterwards it follows a positive slope up to final fracture. The effect of the temperature profile on the electro-mechanical response was also investigated. The on-line recording of the specimen's temperature during the fatigue loading summarized in Figure 5 revealed a rapid increase at the initial stages of loading followed by a steady response till the final fracture for both materials. For each specimen, the experimentally recorded resistance (R_{exp}) is a result of the change of the initial/nominal resistance (R_o) due to temperature ($\Delta R_{thermal}$) and due to damage development (ΔR_{damage}).

$$R_{exp} = R_o + \Delta R_{thermal} + \Delta R_{damage}$$

The expected electrical resistance change due to the temperature can be calculated using the following equation:

$$\Delta R_{thermal} = A \times \Delta T$$

Where (A) is the resistance temperature coefficient expressed in Ohm/°C and ΔT the temperature difference from the starting point ($\Delta T = T - T_0$). The resistance temperature coefficient (A) was experimentally measured to be $-11e^{-5}$ Ohm/°C for the reference composite and $-13e^{-5}$ Ohm/°C for the nanocomposites.

The computed electrical resistance change ($\Delta R_{\text{thermal}}$) was subtracted from recorded value of the resistance in order to obtain the temperature corrected (temperature free) resistance value.

$$(R_0 + \Delta R_{\text{damage}}) = R_{\text{corrected}} = R_{\text{temp-free}} = (R_{\text{exp}} - \Delta R_{\text{thermal}})$$

Figure 6 presents for a random specimen the normalized electrical resistance response ($\Delta R/R_0$) using for the ($\Delta R = R - R_0$) calculation either the experimental (R_{exp}) resistance value or the corrected resistance value ($R_{\text{corrected}}$). As can be seen, the temperature contribution to the ERC was almost negligible. Same behavior is observed for all specimens for both materials.

3.1 Electromechanical response and fatigue damage accumulation

Well established theoretical considerations [13-15] regard the characteristics of fatigue damage development intrinsic to the lay-up of the laminate. However, the rate of damage development depends upon the intensity of the applied fatigue loading (mean stress and variational amplitude) and the loading spectrum. Since the electromechanical response of the composite is strongly connected to damage accumulation, in the case of the fatigue loading the layup of the composite determines the type, the development and the evolution of the damage while the applied load level controls the rate of damage accumulation. Figure 7 summarizes the electrical resistance change versus fatigue life -both in normalized form- for specimens tested at all stress levels, both for the reference (left) and the CNT doped (right) quasi-isotropic CFRP laminates. As can be seen, the normalized fatigue life, where the lower limit of the electrical response was recorded, was observed -independently of the applied stress- within a very narrow range ($NFL_{\text{min}} = 8.66 \pm 3.74$ %). Similar observation was made for the nano-modified material. The respective range of minimum resistance for normalized fatigue life ($NFL_{\text{min}} = 6.84 \pm 2.40$ %) was observed at slightly lower value with narrower range. Additionally in both cases, the upper (maximum) limit of the normalized electrical resistance (resistance variation divided by the initial/nominal resistance) response $(\Delta R/R_0)_{\text{max}}$ was

On the fatigue life prediction of CFRP laminates using Electrical Resistance Change method

recorded always prior to the final fracture. Furthermore in Table 1 the maximum resistance change $(\Delta R/R_o)_{\max}$ is summarized for both material at same stress level. It is observed that $(\Delta R/R_o)_{\max}$ recorded before final fracture is increasing as the applied stress is reduced for both materials.

Moreover the presence of carbon nanotubes tend to moderate the resistance variation prior to the final fracture $(\Delta R/R_o)_{\max}$ especially for increased fatigue duration caused by reduced stress levels.

In Figure 8 the normalized stiffness reduction versus the normalized fatigue life are presented for specimens tested at all stress levels for the reference (left) and the CNT doped (right) CFRP material. According to the literature [13-15] as is depicted in Figure 9 (left) from the aforementioned graphs three (3) main regions of material behavior were approximately identified.

For the reference CFRP laminates: Region I < 7 ± 3 [%] of normalized fatigue life < Region II < 75 ± 5 [%] of normalized fatigue life < Region III. For the CNT doped CFRP laminates: Region I < 7 ± 3 [%] of normalized fatigue life < Region II < 70 ± 10 [%] of normalized fatigue life < Region III.

As reported by Reifsnider et al. [13] and illustrated in Figure 9 (right) the first (I) region of damage development consisted of multiple matrix cracking along fibers in off-axis plies, culminating in a saturation state of cracking in individual plies. This generic pattern of matrix cracking is termed the characteristic damage state (CDS), and is a characteristic of the lay-up of the material. It has been found that this CDS does not depends from variables such as load history and its appearance expressed as percentage of the fatigue life (normalized fatigue life) is independent of the applied load. In the second (II) region, following CDS, the ply cracks link up locally by debonding the ply to ply interface. Further loading cycling causes growth and coalescence of delamination. The final third (III) region of the damage process is characterized by fiber breakage in the longitudinal plies and total failure. It was observed that the transition areas between the regions I to II and II to III were similar for both types of materials. Interestingly enough, the parameter (NFL_{\min}) of the electromechanical response exhibited similar values for the transition areas between regions I and II. On the contrary the transition from region II to region III did not depend on the electromechanical response.

Further analysis of the electromechanical response was performed in order to correlate directly with the modulus drop to the ERC. (Figures 10 and 9, reference and nano-doped CFRP). The analysis revealed that the electrical resistance change ($\Delta R/R_0$) exhibited a monotonic or even linear correlation with the mechanical stiffness reduction following the lower limit $(\Delta R/R_0)_{\min}$ of the relative resistance change. Additionally this lower limit $(\Delta R/R_0)_{\min}$ corresponded to a specific value for the modulus drop as seen in Figure 8; this modulus drop coincided with the transition between region I and II. In order to consistently determine the specific value of the lower limit of the relative resistance change, the experimental curve was fitted using a 4th order polynomial using a least square approximation. The minimum $(\Delta R/R_0)_{\min}$ was defined as the value where the first derivative of the fitted curve is zero. By applying this methodology to all specimens from all stress levels it was observed that the lower limit $(\Delta R/R_0)_{\min}$ coincided with a modulus drop of 0.96 ± 0.01 for the reference material and 0.96 ± 0.02 for the nano-modified material.

All aforementioned observations led to the conclusion that the electrical resistance drop recorded at the initial stages of the fatigue test was directly linked to the multiple matrix-cracking along fibers in off-axis plies taking place during region I. The normalized value of the fatigue life where the lower limit $(\Delta R/R_0)_{\min}$ of the electrical response was recorded (NFL_{\min}) corresponded to the Characteristic Damage State (CDS) of the quasi isotropic laminate.

Although the CDS coincides as percentage of fatigue life to the point where the $(\Delta R/R_0)_{\min}$ appears, the initial decrease of the electrical resistance of the CFRP laminates is not only related to the damage development but has to do with other mechanisms, which are activated during the first stages of the fatigue loading. Among them the increase in the zero degree (0°) of fiber alignment, the fiber piezo-resistive effect, the relaxation of the fiber pre-stressing and the decrease of the contact resistance are attributed to this phenomenon. Those mechanisms are explained in more detail later within Discussion section.

3.2 Parallel use of Acoustic Emission (AE) Results

In Figures 12 and 13 the experimental data from the electrical resistance and modulus drop are shown together with the cumulative number of AE hits against the number of cycles for each

material type. In general, the AE technique is capable of identifying the characteristic damage regions.

In the present study AE activity was monitored by placing one pico AE transducer in the middle of the gauge length of the fatigue samples. The AE sensor used was by Physical Acoustics Corporation (USA) with a frequency range of 100-800 kHz recorded continuous AE activity at a sampling rate of 2 MHz.

In both cases it is observed that during the range of 5 to 10 % of the Fatigue Life, the rate of the AE hits increases significantly. The increase of the AE hits is related with the culminating matrix cracks reaching their saturation point (CDS) and the initiation of the ply interface degradation (stage II). In the same range of the fatigue life, both electrical resistance and modulus drop are indicating the same damage state alternation. The parallel use of AE technique confirmed once more the relation of the electromechanical response with the Characteristic Damage State (CDS) and that the electrical resistance drop recorded at the initial stages of the fatigue test is directly linked with the multiple matrix-cracking along fibers in off-axis plies taking place during region I.

3.3 The electromechanical response for Fatigue Life prediction

The experimental results revealed that the response of the electrical resistance is directly linked with the damage accumulation and more specifically the occurrence of $(\Delta R/R_0)_{\min}$ corresponds to the occurrence of the Characteristic Damage State (CDS). A parameter, that is associated with a specific percentage of stiffness reduction and depends mainly on the composite lamination. Since $(\Delta R/R_0)_{\min}$ occurs at a specific percentage of the fatigue life (NFL_{\min}) independently from the applied load, an initial estimation of the cycles to failure was possible using a ($y=a \times x$) linear equation. The unknown variable (y) is the fatigue life expressed in cycles to failure, the slope constant (a) equals to $a = \frac{1}{NFL_{\min}}$ where $NFL_{\min} = 8.66 \pm 3.74$ % for reference CFRP and $NFL_{\min} = 6.84 \pm 2.40$ % for the nano-composite and the known variable (x) is the fatigue cycles counted till $(\Delta R/R_0)_{\min}$ occurs. Figures 14 and 15 present the theoretical graphs of the fatigue life computed versus the fatigue cycles during electrical resistance lower limit for each material type

(reference and nano-composite). Apart from the theoretical average line the experimental values and the lines that define the statistical range of $1*\sigma=68\%$ are also drawn. It can be seen that the experimental values are very close to the prediction line and most of them are inside the $1*\sigma=68\%$ statistical range area. Additionally, in Figures 16 and 17 a best fit test was performed for the experimental results plotted in the same axis template. The standard allometric power scaling law ($y=a*x^b$) resulted to the highest coefficient of confidence (85% for reference and 91% for nano-composite).

4. Discussion

A reduction of the recorded electrical resistance during initial stages of fatigue was also reported by Schulte et al. [3-4] using a similar electrical measurement setup on orthotropic $[0_2,90_2,0_2,90_2]_s$ CFRP specimens. In that study ($f=10$ Hz, $R=0.1$, $\sigma_{max}=731$ MPa) this reduction was attributed to the temperature increase during the fatigue test since the resistance reduction (1-2 m Ω) was small compared with the total 11.7 \pm 6 m Ω recorded reduction during their study. For the orthotropic $[0_2,90_2,0_2,90_2]_s$ CFRP specimens the temperature recordings showed a 10 $^\circ$ C increase for 10% of the fatigue life with an increasing trend up to 30 $^\circ$ C till final fracture occurred. On the other hand, the quasi-isotropic $[0, +45, 90, -45]_{2s}$ CFRP specimens of this study exhibited an average increase of 3 $^\circ$ C up to 10% of their fatigue life with no further increase till the final fracture.

Chung et al. [16-21] examined the electromechanical fatigue response of orthotropic $[0/90]_n$ CFRP materials. During fatigue tests ($f=1$ Hz, $R=0.05$, $\sigma_{max}=395$ MPa) and at the initial stage of fatigue life (0.1%) the recorded electrical resistance was also reduced. This effect was partially attributed to the irreversible increase in the degree of (0 $^\circ$) fiber alignment. Additionally, the (90 $^\circ$) fiber layers were penetrated by the (0 $^\circ$) wavy fiber layers during composite fabrication. During the initial loading cycles the extent of penetration gradually decreased. This mechanism was also used to explain the electromechanical fatigue behavior of the quasi-isotropic CFRP specimens of this study. However, the gradual decrease of the (0 $^\circ$) fiber penetration was expected to last a very brief period of the fatigue life compared with the reported duration. (8.66 \pm 3.74 %NFL for reference CFRP material and 6.84 \pm 2.40 % for the nano-composite). Another mechanism that was also described as

the possible cause for the electrical resistance drop during initial fatigue stages was the fiber piezoresistive effect, in which the resistivity of the fiber decreased reversibly during the tension of the fiber. This was attributed to the reduction of the residual compressive stress in the fiber inside the polymer matrix composite [22].

In the literature the important issue of the quality of electrical contacts of measuring electrodes on the specimens is also raised [23-31]. The electrode contact resistance (R_c) may result to erroneous experimental electromechanical recordings. Contact resistance (R_c) is inversely proportional of the contact area which is directly linked with the pressure applied on the contacting surfaces. In this study, and as is described in the experimental section, the selected design and construction of the electrodes (high pressure applied via the hydraulic grips of the testing machine) secured that the contact resistance was minimized and kept minimum until fracture. Another parameter that may influence the contact resistance is the temperature. During the experimental calculation of the resistance-temperature correction coefficient which was described in a previous section, the same grip-electrode-specimen setup was employed. This fact secured that the temperature correction calculated in the aforementioned section took into account the influence of the temperature of the specimen on the electrode contact resistance. Finally, the overall temperature effect was negligible, and this observation was made for the total temperature effect that included the probable change of contact resistance and the resistance of the specimen.

Electrical conduction in CFRPs is realized directly through the conductive carbon fibers (CF) since electrical conductivity of the epoxy matrix -even with the addition of CNTs - is several orders of magnitude lower than that of the carbon fibers [11]. Furthermore, the stochastic contact of adjacent fibers creates additional electrical paths for the electric current. The electrical resistance is a parameter that depends on the measurement topology and the shape of the material under investigation. The presence of the (90°) laminas had little effect on the measured resistance of the quasi-isotropic material of this study and the selected volume/bulk electrical resistance measurement topology in the (0°) direction. The electrical conductivity of (90°) laminas at this direction (0°) depends only from stochastically created 90° fiber contacts and is significant lower

than (0°) laminas. Furthermore for the given quasi-isotropic lamination sequence $[0, +45, 90, -45]_{2S}$ intra-laminar fiber contacts of (90°) and ($\pm 45^\circ$) laminas may offer some additional paths for electrical conduction at (0°) electrical conduction. However the influence of this mechanism is limited due to the fact that the ($\pm 45^\circ$) laminas do not offer any direct electrical path since specimen's rectangular shape had high ($\gg 1$) length to width ratio. The analysis of the experimental electrical recordings supports the aforementioned conclusion. Figure 18 presents the variation of the electrical resistance measured at two instances of the fatigue life (35% and 89%). It is observed that the Peak-to-Peak amplitude was constant until final fracture ($\sim 0.3-0.4 \text{ m}\Omega$) despite the optically obvious (90°) delamination. Additionally, as seen in Figures 10 and 11, the recordings of mean –stress/cycle free- electrical resistance after the occurrence of $(\Delta R/R_0)_{\min}$ (damage states II and III) did not present any significant fluctuation. This observation indicated that another damage mechanism may be present apart from the gradual increase of fiber breakages. The lamina clusters of (0°) and ($\pm 45^\circ$) should mainly influence the electrical resistance. The ($\pm 45^\circ$) laminas do not offer any direct electrical path since specimen's rectangular shape has high ($\gg 1$) length to width ratio. But when in contact with (0°) laminas, the off-axis laminas stochastically create (short-circuit type as depicted in Figure 19) electrical paths allowing better electric charge flow translated to lower electrical resistance. The recorded initial resistance (R_0) prior the start of the fatigue load represented an electrical network which comprised the (0°) laminas electrical paths and a given number of (0°) / ($\pm 45^\circ$) short-circuits. This network was formed during the composite manufacturing stage due to the pressure applied to the composite forcing the laminates to compact. As fatigue loading initiated and multiple matrix-cracking along fibers in off-axis plies is developed, the probability of fiber contact increased since any crack developed destroyed the insulating matrix layer between neighboring fibers allowing possible contact. This increased likelihood is translated in greater number of the stochastically created (0°)/($\pm 45^\circ$) short-circuits and the drop the electrical resistance was observed. As the matrix cracking mechanism saturated, the electrical short-circuit mechanism ceased to take place. Afterwards, the systematic failure of the CF gradually increased, leading to the respective loss of direct electrical paths and consequentially to the increase of the

On the fatigue life prediction of CFRP laminates using Electrical Resistance Change method

electrical resistance. The deterioration rate of the $(0^\circ)/(\pm 45^\circ)$ interply interface –directly linked with short-circuit mechanism- controlled the increase rate of the electrical resistance by offering alternative electrical paths when the (0°) paths were destroyed. The aforementioned electromechanical mechanism is proposed as the major –but not the sole- mechanism causing the observed resistance drop. The electrical network created for the 16 plies of the quasi-isotropic lamination is too complex and an analytic calculation via a resistor network theory is needed to verify the “window” where the aforementioned mechanism is dominant.

The use of the electrical response for the prediction of the fatigue life was also proposed by P.E Irving et al. [32]. They performed fatigue experiments at a given stress level of unidirectional $[0]_{16}$ CFRP specimens and recorded the (0°) resistance. They correlated resistance changes occurring early in the fatigue life (1000 cycles) of a sample with the eventual life, as the basis of a life estimation technique for in-plane fatigue. Jung-Ju Lee et al. [33] also investigated the electrical resistance change as a damage parameter of fatigue damage such as the degradation of residual strength and stiffness. They observed a very similar trend of change between the measured stiffness and electrical resistance change during fatigue tests. They used this change in electrical resistance as a damage parameter on the basis that cumulative fatigue damage was manifested via the degradation of residual stiffness and by the change in electrical resistance. They also tried to predict the damage accumulation for composite laminates subjected to fatigue loading using an electrical resistance damage model interlinked a stiffness degradation model. The predicted value showed good agreement with the experimental data. Finally the electrical resistance damage parameter together with stiffness reduction during fatigue was investigated using a neural network. The predicted values showed good correlation with the experimental results. Additional studies [34-35] compared the ERC method with a more classical non-destructive technique such as Acoustic Emission. They verified that the electrical resistance measurement allowed in-situ monitoring of the evolution of various internal damage nucleation and growth in CFRP such as fiber fractures, intraply matrix cracks and interply delaminations. Other studies [36-37] also verified the correlation of electrical resistance with stiffness degradation and proposed that critical changes of resistance or

capacitance variation could be a warning for the structural integrity during cyclic loading, introducing thus a health monitoring approach. Furthermore the strong dependence of the DC and AC electrical properties upon the electrical fiber to fiber contacts was verified and resistor network theory was applied [38-39]. Finally analytical and numerical electro-mechanical models [40-44] were developed to predict the electrical resistance change in unidirectional fiber reinforced composite materials.

5. Conclusions

This paper studied for first time the electromechanical response to fatigue loading conditions of quasi-isotropic composites. Furthermore the effect of dispersed Multi-Wall Carbon NanoTubes (MWCNT) in the matrix was additionally evaluated and compared with neat epoxy CFRPs. The analysis of the experimental results suggested that the fatigue response of the electrical resistance was dominated by different electromechanical damage mechanisms than the unidirectional and orthotropic [0/90] CFRP materials. In the case of the (0°) electrical resistance the reduction observed for a significant part of the fatigue life (~10%) was attributed to an electrical short-circuit mechanism controlled by the presence of the [±45] laminas linked with the matrix deterioration. Mechanisms such as the reduction of the residual stresses on the fiber bundles and the partially irreversible increase in the degree of (0°) fiber alignment should also be considered. With the onset of the stochastic failure of the (0°) carbon fibers along with the crack coupling and the interfacial deponding, the short-circuit mechanism offers alternative electrical paths as the (0°) paths are destroyed. As delaminations start, the destruction of the direct (0°) electrical paths becomes dominant and governs the electrical response until specimen failure. The coupling between the responses of the electrical resistance, the mechanical stiffness and acoustic emission verified the aforementioned conclusions and also led to the important observation that the Characteristic Damage State (CDS) was directly linked the lower limit of the electrical change ($\Delta R/R_{0\min}$). This observation allowed for the prediction of the fatigue life with considerably high degree of confidence, assuming a constant stress level throughout the whole lifetime.

The presence of the MWCNT in the epoxy matrix for carbon fiber based composites did not alter drastically the electrical response, especially for the specific measurement topology and material lamination. Despite the fact that the CNT addition increases the electrical conductivity of the matrix by many orders of magnitude, the effect is masked by the presence of the conductive carbon fibers. As a result, the nano-doped matrix did not contribute directly to the electrical conduction mechanism. Nevertheless in microscopic level, the presence of the nanotube influenced positively the mechanism of fiber to fiber electrical contact. During fatigue the range of the electrical resistance change ($\Delta R/R_0$) for the nano-doped CFRP specimens exhibited a decreasing trend. Additionally, the fatigue life prediction the nanocomposites had higher coefficient of confidence (R^2)

Acknowledgments

The financial support of the FP6 EU-STREP project NOESIS is acknowledged. This research project is co-financed by E.U.-European Social Fund (75%) and the Greek Ministry of Development-GSRT (25%).

REFERENCES

- [1] Todoroki A, Ueda M, Hirano Y. Strain and Damage Monitoring of CFRP Laminates by Means of Electrical Resistance Measurement. *Journal of Solid Mechanics and Materials Engineering*; 2007; 1(8): 947-974.
- [2] Chung D.D.L. Damage detection using self-sensing concepts. *Proceedings of the Institution of Mechanical Engineers, Part G: Journal of Aerospace Engineering*; 2007; 221(4): 509-520.
- [3] Baron C, Schulte K. Determination of electric resistance for in-situ determination of fibre failure in carbon fibre-reinforced plastic composites. *Material-pruefung*; 1988; 30(11-12): 361-366.
- [4] Schulte K, Baron C. Load and failure analyses of CFRP laminates by means of electrical resistivity measurements. *Composites Science and Technology*; 1989; 36(1): 63-76.
- [5] Thostenson E, Renb Z, Choua T.W. Advances in the science and technology of carbon nanotubes and their composites: a review. *Composites Science and Technology*; 2001; 61:1899-1912
- [6] Popov N.V. Carbon nanotubes: properties and application. *Materials Science and Engineering*; 2004; R43: 61-102
- [7] Robertson J. Realistic application of CNTs. *Materials Today*; 2004; 7: 46-52
- [8] Kostopoulos V, Tsotra P, Vavouliotis A, Karapappas P, Tsantzalis S, Loutas T. Nano-modified fiber reinforced composites: A way towards the development of new materials for space applications. *Proc. of 5th ESA Symp. on Micro/Nano Technologies for Space, ESTEC, Noordwijk (ESA-WPP-255) 2005.*
- [9] Kostopoulos V, Tsotra P, Vavouliotis A, Karapappas P, Tsantzalis S, Loutas T. Damage detection during fatigue of CNF doped CFRPs via resistance measurements and AE. *Solid State Phenomena*; 2007;121-123:1399-1402

- [10] Kostopoulos V, Vavouliotis A, Karapappas P, Tsotra P, Paipetis A. Damage monitoring of carbon fiber reinforced laminates using resistance measurements. Improving sensitivity using carbon nanotube doped epoxy matrix system. *Journal of Intelligent Material Systems and Structures*; 2009; 20(9): 1025-1034.
- [11] Vavouliotis A, Karapappas P, Loutas T, Voyatzi T, Paipetis A, Kostopoulos V. Multistage fatigue life monitoring on carbon fibre reinforced polymers enhanced with multiwall carbon nanotubes; *Plastics, Rubber and Composites*; 2009; 38(2-4): 124-130.
- [12] Barkoula N.M, Paipetis A, Matikas T, Vavouliotis A, Karapappas P, Kostopoulos V. Environmental degradation of carbon nanotube-modified composite laminates: A study of electrical resistivity. *Mechanics of Composite Materials*; 2009; 45(1): 21-32.
- [13] Case S.W, Reifsnider K.L. *Fatigue of Composite Materials*; Chapter 4.16. 2007; 405-441.
- [14] Talreja R. *Fatigue of Polymer Matrix Composites*, *Comprehensive Composite Materials*; Chapter 2.14. 2000; 529-552.
- [15] Talreja R. Multi-scale modeling in damage mechanics of composite materials. *Journal of Materials Science* 2006; 41(20):6800–6812.
- [16] Chung D.D.L. Self-monitoring structural materials. *Materials Science and Engineering Reports* 1998; 22(2): 57-78.
- [17] Wang X, Chung D.D.L. Self-monitoring of fatigue damage and dynamic strain in carbon fiber polymer-matrix composite. *Composites Part B: Engineering* 1998; 29: 63-73.
- [18] Wang X, Wang S, Chung D.D.L. Sensing damage in carbon fiber and its polymer-matrix and carbon-matrix composites by electrical resistance measurement. *Journal of Materials Science* 1999; 34: 2703-2713.
- [19] Wang S, Shui X, Fu X, Chung D.D.L. Early fatigue damage in carbon-fibre composites observed by electrical resistance measurement. *Journal of Materials Science* 1998; 33: 3875-3884.

- [20] Wang X, Chung D.D.L. Real-time monitoring of fatigue damage and dynamic strain in carbon fiber polymer-matrix composite by electrical resistance measurement. *Smart Materials and Structures* 1997; 6: 504-508.
- [21] Chung D.D.L, Wang S. Self-sensing of damage and strain in carbon-fiber polymer-matrix structural composites by electrical resistance measurement. *Polymers and Polymer Composites* 2003; 11: 515-525.
- [22] Wang X, Chung D.D.L. Residual stress in carbon fiber embedded in epoxy, studied by simultaneous measurement of applied stress and electrical resistance. *Composite Interfaces* 1998; 5(3): 277-281.
- [23] Khemiri N, Angelidis N, Irving PE. Experimental and finite element study of the electrical potential technique for damage detection in CFRP laminates. *Experimental and finite element. Smart Materials and Structures* 2005;14: 147-154.
- [24] Angelidis, N., Wei, CY. και Irving, PE. The electrical resistance response of continuous carbon fibre composite laminates to mechanical strain. *Composites Part A* 2004; 35: 1135-1147.
- [25] Chung, D.D.L. και Wang, S. Discussion on paper 'The electrical resistance response of continuous carbon fibre composite laminates to mechanical strain' by N. Angelidis, C.Y. Wei and P.E. Irving, *Composites: Part A* 35, 1135-1147 (2004). *Composites Part A: Applied Science and Manufacturing* 2006; 37: 1490-1494.
- [26] Angelidis, N, Wei, C.Y. και Irving, P.E. Response to discussion of paper: The electrical resistance response of continuous carbon fibre composite laminates to mechanical strain. *Composites Part A: Applied Science and Manufacturing* 2006; 37: 1495-1499.
- [27] Wang, S. και Chung, D.D.L. Piezoresistance in continuous carbon fiber polymer-matrix composite. *Polymer Composites* 2000;21: 13-19.
- [28] Todoroki, A. και Yoshida, J. Electrical resistance change of unidirectional CFRP due to applied load. *3. JSME Int. J. Series A* 2004; 47:357-364.

- [29] Todoroki, A. και Yoshida, J. Apparent negative piezoresistance of single-ply CFRP due to poor electrical contact of four probe method. *Key Engineering Materials* 2005; 610-615.
- [30] Sirong, Z. και Chung, D.D.L. Analytical model of piezoresistivity for strain sensing in carbon fiber polymer–matrix structural composite under flexure. *Carbon* 2007; 45: 1606-1613.
- [31] Todoroki, A., Tanaka, M. και Shimanura, Y. Measurement of orthotropic electric conductance of cfrp laminates and analysis of the effect on delamination monitoring with an electric resistance change method. *Composite Science and Technology* 200; 62: 619-628.
- [32] Irving, P.E. και Thiagarajan, C. Fatigue damage characterization in carbon fibre composite materials using an electrical potential technique. *Smart Materials and Structures* 1998; 7: 456-466.
- [33] Dae-Cheol Seo, Jung-Ju Lee. Damage detection of CFRP laminates using electrical resistance measurement and neural network. *Composite Structures, Tenth International Conference on Composite Structures 1-4, December 1999*;47: 525-530.
- [34] Ceysson, O., Salvia, M. και Vincent, L. Damage mechanisms characterization of carbon fibre/epoxy laminates by both electrical resistance measurements and acoustic emission analysis. *Scripta Materialia* 1996; 34: 1273-1280.
- [35] Prasse T, Michel F, Mook G, Schulte K, Bauhofer W. A comparative investigation of electrical resistance and acoustic emission during cyclic loading of CFRP laminates. *Composites Science and Technology* 2001; 61(6):831-835.
- [36] Abry J.C, Choi Y.K, Chateauinois A, Dalloz B, Giraud G. and Salvia M. In-situ monitoring of damage in CFRP laminates by means of AC and DC measurements. *Composites Science and Technology*; 2001; 61(6): 855-864.
- [37] Abry J.C, Bochart S, Chateauinois A, Salvia M, Giraud G. In situ detection of damage in CFRP laminates by electrical resistance measurements. *Composites Science and Technology* 1999; 59(6): 925-935.

- [38] Kupke M, Schulte K, Schuler R. Non-destructive testing of FRP by d.c. and a.c. electrical methods. *Composites Science and Technology* 2001; 61(6): 837-847.
- [39] Weber I, Schwartz P. Monitoring bending fatigue in carbon-fibre/epoxy composite strands: a comparison between mechanical and resistance techniques. *Composites Science and Technology* 2001; 61(6): 849-853.
- [40] Park J.B, Okabe T, Takeda N. New concept for modeling the electromechanical behavior of unidirectional carbon-fibre-reinforced plastic under tensile loading. *Smart Materials. Structures* 2003; 12:105-114.
- [41] Park J.B, Okabe T, Takeda N, Curtin WA. Electromechanical modeling of unidirectional CFRP composites under tensile loading condition. *Composites Part A: Applied Science and Manufacturing* 2002; 33: 267-275.
- [42] Park J.B, Lee S, Kim KW, Yoon DJ. Interfacial Aspect of Electrodeposited Conductive Fibers/Epoxy Composites Using Electro-Micromechanical Technique and Nondestructive Evaluation. *Journal of Colloid and Interface Science* 2001; 237(1): 80-90.
- [43] Xia ZH, Curtin WA. Modeling of mechanical damage detection in CFRPs via electrical resistance. *Composites Science and Technology* 2007; 67(7-8): 1518-1529.
- [44] Xia ZH, Curtin WA. Damage detection via electrical resistance in CFRP composites under cyclic loading. *Composites Science and Technology* 2008; 68(12): 2526-2534.

Figure Captions

Figure 1	Test specimen geometry, electrode and thermocouple setup and location.
Figure 2	Central Logging System overview (On-line Parallel Monitoring of electrical resistance, temperature, load, displacement, time, etc)
Figure 3	Graph of specimen's electrical resistance and applied load versus time and fatigue cycles
Figure 4	Mean –stress/cycle free- electrical response versus fatigue time in loading cycles.
Figure 5	Graph of Temperature variation versus normalized fatigue life.
Figure 6	Graph of electrical resistance change normalized with initial value R_0 versus fatigue life also normalized. Experimental and temperature corrected results are presented. Inset graph: Temperature profile during fatigue.
Figure 7	Normalized electrical resistance change versus normalized fatigue life for various specimens of all stress levels.
Figure 8	Stiffness reduction (modulus drop) versus the fatigue life –both in normalized form- for various specimens of all stress levels.
Figure 9	(Left) Experimental stiffness loss, normalized to the first cycle stiffness, for a $[+45/0/-45/90]_{2S}$ composite laminate subjected to fatigue loading conditions. [14-15] (right) Stages of damage development in the lifetime of a composite material [14-15]
Figure 10	Normalized Electrical resistance change versus modulus drop for reference quasi-CFRP material. Experimental values and polynomial fitting.
Figure 11	Normalized Electrical resistance change versus modulus drop for CNT-doped quasi-CFRP material. Experimental values and polynomial fitting.
Figure 12	Cumulative number of Acoustic Emission hits versus normalized fatigue life for reference quasi-CFRP material. Also in double axis format normalized electrical resistance and modulus drop.
Figure 13	Cumulative number of Acoustic Emission hits versus normalized fatigue life for CNT-doped quasi-CFRP material. Also in double axis format normalized electrical resistance and modulus drop.
Figure 14	Fatigue life prediction line versus the fatigue cycles during electrical resistance lower limit for reference quasi-CFRP material.
Figure 15	Fatigue life prediction line versus the fatigue cycles during electrical resistance lower limit for CNT-doped quasi-CFRP material.
Figure 16	Standard allometric power scaling law fitting ($y=a \times x^b$) of experimental data of fatigue life versus the fatigue cycles during electrical resistance lower limit for reference quasi-CFRP material.
Figure 17	Standard allometric power scaling law fitting ($y=a \times x^b$) of experimental data of fatigue life versus the fatigue cycles during electrical resistance lower limit for CNT-doped quasi-CFRP material.
Figure 18	On-line response of electrical resistance and load versus fatigue cycles at 35% (right) and 89% (left) of fatigue life.
Figure 19	Illustration of $(0^\circ)/(\pm 45^\circ)$ short circuit conduction mechanism

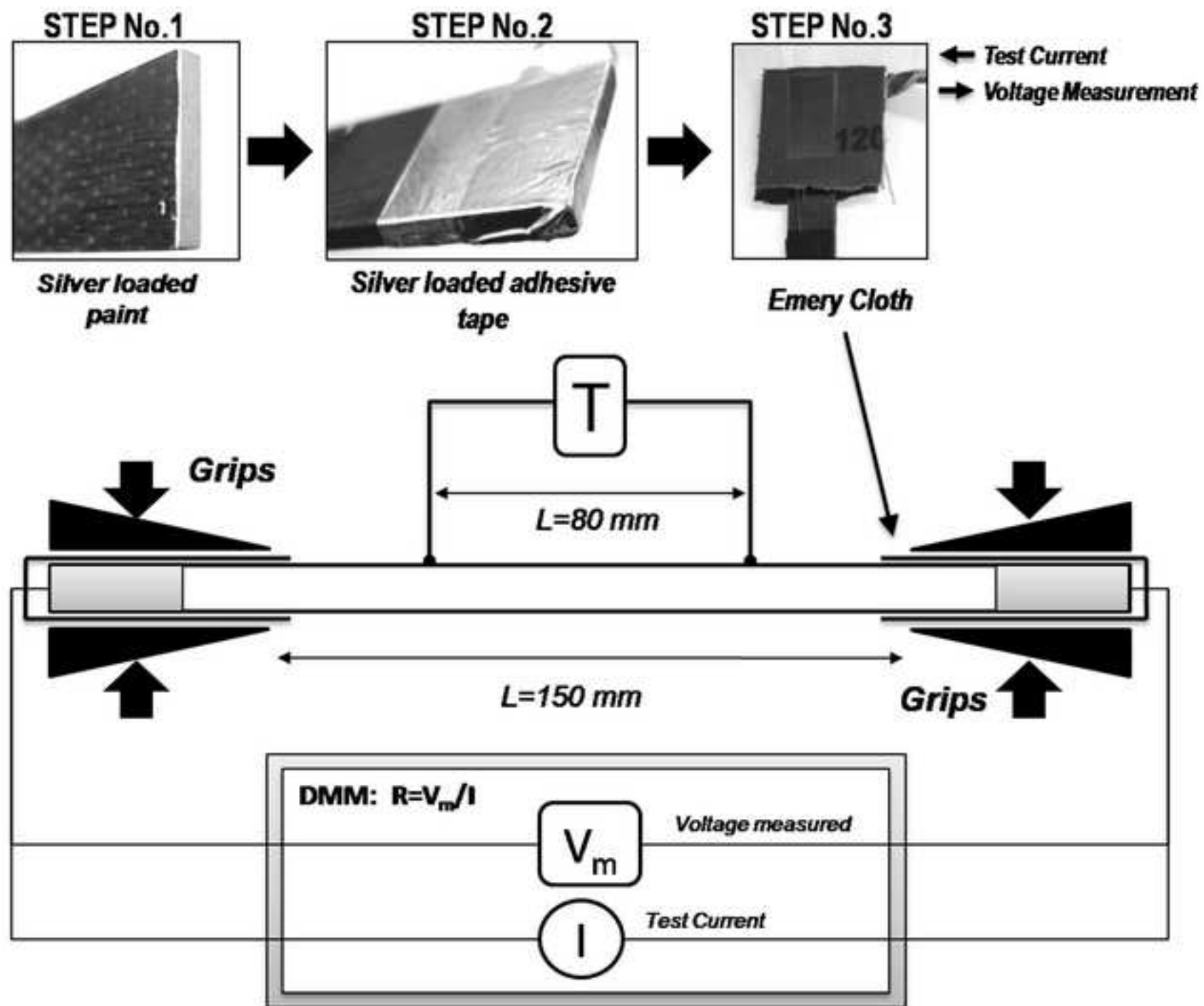
Table Captions

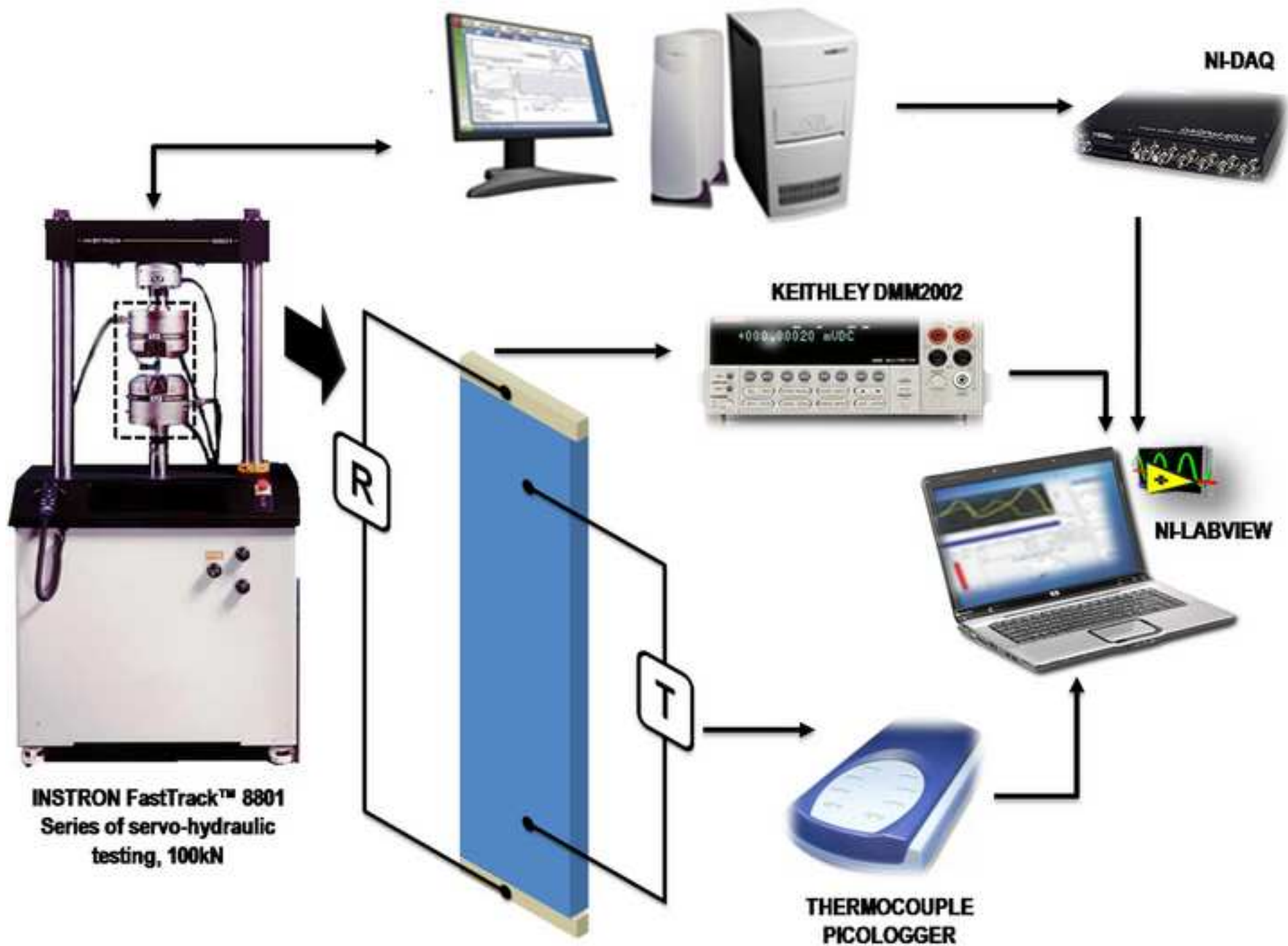
Table 1	Maximum resistance change $(\Delta R/R_0)_{\max}$ for both material at stress levels 1 and 3..
---------	--

Tables

Stress Level	Material	$(\Delta R/R_0)_{\max}$
1 (80% of σ_{uts})	Reference quasi-isotropic CFRP	5,66±2,86 [%]
	CNT doped quasi-isotropic CFRP	5,59±2,27 [%]
3 (60% of σ_{uts})	Reference quasi-isotropic CFRP	17.06±4.76 [%]
	CNT doped quasi-isotropic CFRP	10.23±1.62 [%]

Table 1





Time [sec]

